MICROCHEMICAL JOURNAL 50, 413–433 (1994)

Laser-Induced Breakdown of Metal Vapor

V. I. MAZHUKIN,* I. V. GUSEV,* I. SMUROV,† AND G. FLAMANT‡

*Institute of Mathematical Modeling, Russian Academy of Science, Miusskaya Square 4, 125047 Moscow, Russia; †Ecole Nationale d'Ingénieurs de Saint-Etienne, 58 rue Jean Parot, 42023 Saint-Etienne Cédex 2, France; and ‡Institut de Science et de Génie des Matériaux et Procédés, C.N.R.S. B.P. No. 5, 66125 Font-Romeu Cédex, France

Received and accepted July 17, 1994

The interaction of laser radiation in the intensity range $G = 10^6 \div 10^{10}$ W/cm^2 and at the wavelength $\lambda = 1.06$ μm with copper vapor is simulated, using a collision—radiation model describing the kinetics of nonequilibrium ionization and recombination. It is shown that the interaction of laser radiation with vapor can proceed in two qualitatively different ways, namely, prebreakdown and optical breakdown regimes. If the radiation intensity is insufficient to induce avalanche ionization, the system transfers to a stationary state characterized by one temperature, the equilibrium between the radiation and the vapor being absent. For higher values of laser intensity, optical breakdown starts, i.e., the nonequilibrium transition state from a partially ionized vapor to a fully ionized plasma where Coulomb collisions are predominant. Simulations confirm experimental results that optical breakdown refers to a distinct threshold in the radiation intensity. In the macroscopic description of breakdown, the threshold intensity values depend on the ionization potential and the electronic state distribution of neutral atoms as well as on the initial temperature of the evaporated material and the laser pulse width.

INTRODUCTION

In the past few years nonequilibrium low-temperature ($T < 10$ eV) laser plasmas have found new fields of applications, e.g., surface treatment of solids (*1, 2*), microelectronics (*3, 4*), processes of reduction of nonorganic compounds, powder metallurgy (*5*), and plasmochemical problems (*6*). In a number of applications low-temperature laser plasmas are used as a high-enthalpy energy source, a source of positive or negative ions (for ion–molecular reactions), and a powerful energy source with controllable spectrum of radiation (for photochemical reactions).

Monitoring and control of laser-induced processes in condensed and gaseous media can be performed in different ways. Diagnosis based on the parameters of low-temperature laser plasma (or plume) has a significant place among them (*7*). The principal objective here is to determine the charge composition and particle energy distribution. The main difficulty results from the fact that laser plasmas come under the heading of an open system and in general are in nonequilibrium because of the presence of an external energy source (in the present case, laser radiation). It is well known that nonequilibrium phenomena are among the most complicated to investigate because of the difficulty of defining a unique temperature for the whole system: the temperature can be introduced only for separate subsystems having Maxwell–Boltzmann distribution.

The typical nonequilibrium laser plasma generated by pulsed laser radiation at

wavelength $\lambda = 1.06$ μm with intensity $G \leq 10^9$ W/cm^2 is characterized by the following physical parameters: For an initial density equal to 10^{16}–10^{21} cm^{-3}, the degree of ionization, α, reaches the value 10^{-4}–1, and the average electron energy, $\epsilon_e = 3kT_e/2$, is equal to 1.0–25 eV, about one order of magnitude above the average translation energy of heavy particles (atoms and ions).

Under laser irradiation, the plasma nonequilibrium is a result of its significant overheating, i.e., the change composition (or the concentration of electrons, ions, and atoms in ground and exited states) will greatly exceed the Saha–Boltzmann distribution (related to temperature, T_g).

There is a considerable amount of experimental and theoretical data on pulsed action of moderate intensity $G = 10^6$–10^{10} W/cm^2 and relatively long duration $\tau = 10^{-9}$–10^{-6} s on different materials over a wide range of wavelengths ($\lambda = 0.238$–10.6 μm) (*8–21*). On the fundamental side, the phenomenon of optical breakdown is related to the general problems of emergence and evolution of highly nonequilibrium systems during the interaction of concentrated energy fluxes with matter. One of the central problems at present with no general solution is the process of establishing local thermodynamical equilibrium in a laser plume. A plasma in the state of a thermodynamic equilibrium is fully determined by its temperature T and density ρ, and its charge composition corresponds to the Saha–Boltzmann distribution. In the case of a violation of the local thermodynamic equilibrium, the plasma behavior is determined by a combination of kinetic, radiative, and gas dynamic processes.

The general complex mathematical modeling of laser plasma formation and development in a gaseous medium could be obtained only in the framework of nonequilibrium radiative gas dynamics (NERADGASDYN). This theory is not yet completed, but it is in the stage of intensive development. The main feature of the NERADGASDYN is the simultaneous consideration of processes at macro- and microlevels (i.e., kinetics at the atomic scale with energy and mass transfer governing the flow structure) occurring under conditions where themodynamic equilibrium is violated.

From the mathematical point of view, the NERADGASDYN consists of three correlated units: gas dynamics, radiation transfer, and collision-radiation kinetics. Each unit is described by the system of partial differential equations: gas-dynamic equations, the multidimensional radiation transfer equation for continuous spectrum, and the integrodifferential equation for linear spectrum radiation transfer (Biberman–Holstein equation), kinetic equations for ionization, recombination, excitation, etc. processes.

To simplify the problem of laser plasma simulation, several stages are usually distinguished. In the present work the initial stage, known as optical breakdown, is considered. The main aim is to analyze the role of nonequilibrium phenomena when kinetic processes dominate and when transfer and diffusion are insignificant. Kinetics of ionization-recombination processes in metal vapor are analyzed based on the collision-radiation model. The prebreakdown regime and the avalanche ionization of copper vapor (as an example) under the laser radiation are simulated.

The process of intensive evaporation of a metal target in to vacuum under

pulsed laser action is considered. Under these conditions the highest temperature and density values of vapor exist at the edge of the Knudsen layer (*30*). Here the probability of optical breakdown is the highest. Hence, it is reasonable to take the above-mentioned values of the vapor's temperature (T_0) and density ($\rho_0 = MN_0$, M is mass of atom) as the initial ones to simulate optical breakdown. Note, that the parameters of the Knudsen layer are determined from the surface temperature T_s.

STATEMENT OF THE PROBLEM

In the present simulation it is assumed that the metal vapor appears as a result of the target evaporation into vacuum under the action of a laser pulse. According to conventional concepts, intensive surface evaporation can be described using the approximation of the Knudson nonequilibrium layer adjacent to the surface being evaporated. Macroscopically, the Knudsen layer is a gas-dynamical gap, at which the main parameters, i.e., the temperature T, the density ρ, and the pressure P of the medium assumed, undergo a discontinuous change. Vapors passing through the Knudsen layer are assumed to be in an equilibrium state. Initial concentrations of electrons and ions in the ground and excited states are determined from the Saha–Boltzmann equations.

On the other hand, the peculiarities of laser-inducted surface evaporation are not considered in the details. The parameters of flow of evaporated metal are used as a basis for the estimation of the initial values of temperature T_0. The range of T_0 and ρ_0 values (determined through the surface temperature T_s of the laser-evaporated target) corresponds to the intensive evaporation of copper (T_s about boiling point at the normal condition). Therefore a Maxwell–Boltzmann distribution may be applied to all the subsystems.

At the initial stage, as a rule, the electron concentration turns out to be too low for a considerable amount of the incident radiation to be absorbed. Later, with a sufficient radiation intensity, the conditions for the avalanche ionization, i.e., the optical breakdown, in the material vapor can be satisfied by the electron gas being heated due to the inverse-bremsstrahlung effect.

Unsteady-State Collision-Radiation Model

There are two important facts to be accounted for by the collision—radiation model describing the dynamics of laser plasma. The first one is the violation, at some stages, of the local thermodynamical equilibrium. This may occur both during the action of the laser pulse and at the completion of the pulse. During the action of the laser pulse, the temperature of electrons (T_e) becomes different from the temperature of atoms and ions (T_g) due to radiation absorption by electrons and to the significant difference of electrons and heavy particles masses. As regards ionization, the produced plasma turns out to be nonequilibrium. In such a state the average charge of the plasma is smaller than that of equilibrium, and the concentration of charged particles and excited states differs (by being smaller) from the Saha–Boltzmann distribution (*31*).

On completion of the laser action, at the stage of the gas-dynamical scattering at a sufficiently high velocity, the plasma may become recombinationally non-

equilibrium (*32*). In this state the relations characterizing the degree of deviation from equilibrium will be inverse as compared on the state discussed above.

Therefore the collision–radiation model describing the behavior of laser plasma must include, in addition to the kinetics equation, two equations for the energy balance: for the electrons and for the heavy particles in the system.

The second fact to be taken into account when constructing the mathematical model is that in metals, as a rule, energy levels of atoms and ions are split and mixed. Therefore when describing the level kinetics in metal vapors it is necessary to take into consideration a great number of excited levels and collision—radiation transitions between them.

The main assumptions are as follows:

1. A monatomic plasma of one chemical element is considered.
2. In the initial state, metal vapors consist of atoms, ions, and electrons which are in the state of complete thermodynamical equilibrium.
3. The stage of free gas-dynamical scattering of plasma is assumed; its initial temperature and density correspond to the ones at the edge of the Knudsen layer for the given surface temperature T_s.
4. Spatial effects are not considered.
5. In the regimes under study the average electron energy does not exceed 10–20 eV. Therefore when constructing the collision—radiation model, metal ions whose ionization potentials greatly exceed this energy range are not taken into consideration.

In the electron configuration of a copper atom, at the unfilled shell $1s^2 2s^2 2p^6 3s^2 3p^6 3d^{10} 4s$ ($^2S_{1/2}$), there is one electron with the ionization potential $I_1 = 7.72$ eV. Then there is the *d*-shell whose outer electrons have comparatively low potentials, $I_2 = 20.291$ eV, $I_3 = 36.834$ eV.

However, electron transitions of the *d*-shell are characterized by a low radiating capacity and their radiative and collisional characteristics are poorly known. For this reason the collision-radiation model of the copper atom includes the kinetics of the neutral Cu atom and the first ion Cu^+ ($z = 1$). The second ion Cu^{2+} ($z = 2$) with $I_2 = 20.291$ eV is included in the model in the form of a nucleus (core).

Elementary Phenomena and Atom Transitions

The major elementary phenomena taken into account in the collision-radiation model are listed below:

(a) Spontaneous radiative decay of excited states of atoms and ions [z – charge state] (*51–53*)

$$A_n^z \xrightarrow{(a_{mn}^z)} A_m^z + \hbar\omega, \tag{1}$$

where a_{mn}^z [s^{-1}] is the constant of radiative transition rate.

(b) Excitation and deexcitation of atoms and ions by an electron impact (*50, 51*).

$$A_n^z + e \underset{k_{nm}^z}{\overset{k_{mn}^z}{\rightleftarrows}} A_m^z + e, \tag{2}$$

where k^z_{mn} [cm$^3 \cdot$ s^{-1}] is the excitation rate constant for electron impact excitation of a particle of charge z in the nth state to the mth state; k^z_{nm} is the deexcitation rate of the mth level.

(c) Ionization of ground and excited states of atoms and ions by an electron impact (*48, 49*).

$$A^z_n + e \xrightarrow{\alpha^z_n} A^{z+1}_0 + e + e, \tag{3}$$

where α^z_n [cm$^3 \cdot$ s^{-1}] is the ionization rate constant of the nth level particle with the z-charge, the ionization being effected by an electron impact.

(d) Three-particle recombination, i.e., a reaction inverse to the impact ionization. The third particle is an electron (*31*).

$$A^{z+1}_0 + e + e \xrightarrow{\beta^z_n} A^z_n + e, \tag{4}$$

where β^z_0 [cm$^6 \cdot$ s^{-1}] is the reaction rate constant.

Table 1 represents the ground and excited state of Cu neutral atoms and ions taken into account by the model. Figures 1 and 2 show collison and radiative transitions between these states.

System of Equations

The charge composition of plasma and level-by-level kinetics of neutral atoms and ions (see Figs. 1 and 2) is described by the following system of nonlinear differential equations: For ground states of neutral atoms ($z = 0$),

$$\frac{\partial N^0_0}{\partial t} = \left[N_e \sum_j (k^0_{j0} N^0_j - k^0_{0j} N^0_0)\right]_{j \in \Omega^0_0} + \left[\sum_{j>0} a^0_{0j} N^0_j\right]_{j \in \Omega^0_0} + \beta^0_0 N^1_0 N_e N_e - \alpha^0_0 N^0_0 N_e. \tag{5}$$

For ground states of z-charged ions ($z \in \{1 \ldots z_{max} - 1\}$),

$$\frac{\partial N^z_0}{\partial t} = \left[N_e \sum_j (k^z_{j0} N^z_j - k^z_{0j} N^z_0)\right]_{j \in \Omega^z_0} + \left[\sum_{j>0} a^z_{0j} N^z_j\right]_{j \in \Omega^z_0} + \left[\sum_j (\alpha^{z-1}_j N^{z-1}_j N_e - \beta^{z-1}_j N^z_0 N_e N_e)\right]_{j \in \Theta^{z-1}} + \beta^z_0 N^{z+1}_0 N_e N_e - \alpha^z_0 N^z_0 N_e. \tag{6}$$

For excited states of neutral atoms and ions ($z \in \{0 \ldots z_{\max} - 1\}$),

$$\frac{\partial N^z_n}{\partial t} = \left[N_e \sum_j (k^z_{jn} N^z_j - k^z_{nj} N^z_n)\right]_{j \in \Omega^z_n} - \alpha^z_n N^z_n N_e + \left[\sum_{j>n} a^z_{nj} N^z_j - \sum_{j<n} a^z_{jn} N^z_n\right]_{j \in \Omega^z_n} + \beta^z_n N^{z+1}_0 N_e N_e, \qquad n \in \Theta^z. \tag{7}$$

For ions with $z = z_{\max}$,

$$\frac{\partial N_0^{z_{\max}}}{\partial t} = \left[\sum_j \alpha_j^{z_{\max}-1} N_j^{z_{\max}-1} N_e - \sum_j \beta_j^{z_{\max}-1} N_0^{z_{\max}} N_e N_e\right]_{j\in\Theta z_{\max}-1}. \tag{8}$$

For electrons,

$$\frac{\partial N_e}{\partial t} = \sum_{z=1}^{z_{\max}} \sum_{i\in\Theta^z} \frac{\partial N_i^z}{\partial t}, \tag{9}$$

where Θ^z is the set of all the considered discreet electron states of the z-charged particle; Ω_i^z is the subset of j states for z particle with $(j - i)$ transition been taken into account. Such transitions of Cu are shown in Figs. 1 and 2. N_i^z is the density of the z-charged particles in the ith state; N_e is the density of free electrons; $z_{\max}$ is the maximum degree of ionization of a neutral atom.

For Cu vapors $z_{\max} = 2$; the particle having the maximum ionization degree is taken to have no structure, i.e., its excited states are neglected.

From the viewpoint of the energy exchange, in the low-temperature monatomic plasma it is possible to distinguish three subsystems: (i) excitation of the electronic energy levels of the atoms and ions and translational degrees of freedom of (ii) the electrons and (iii) the heavy particles. Within each subsystem the energy exchange proceeds most rapidly. Translational energy between electrons and heavy particles is slow due to the great difference between the mass of an electron and that of a heavy particle (an atom or an ion). Consequently, it is only a small portion of kinetic energy of colliding particles that can be transmitted by one collision (*34*):

$$\delta \simeq \frac{2m}{M}(T_e - T_g).$$

Therefore, for the significant number of collisions, the energy balance of the nonequilibrium plasma is characterized by two temperatures: T_e for the electronic component and T_g for heavy particles.

Equations for the energy balance of translational degrees of freedom of electrons and heavy particles are written in the following form (*34*).

$$\frac{d}{dt}\left(\frac{3}{2}N_e T_e\right) = \left\{G\mu - \frac{3}{2}\delta\right\}(\nu_{en} + \nu_{ei})N_e + \sum_{z=0}^{z_{\max}}\left[\sum_n (Q_n^z + \hat{Q}_n^z)\right]_{n\in\Theta^z} \tag{10}$$

$$N_g \frac{d}{dt}(T_g) = \delta(\nu_{en} + \nu_{ei})N_e. \tag{11}$$

The parameter μ characterizes the energy portion gained by the electron in the laser radiation electromagnetic field during one collision with an atom or an ion.

$$\mu = \frac{4\pi e^2}{mc(\omega^2 + (\nu_{en} + \nu_{ei})^2)}.$$

Here $\omega = 2\pi\nu$ is the incident radiation frequency, ν_{en} is the frequency of the electron-neutral collisions; ν_{ei} is the frequency of electron-ion collisions; m, the mass of the electron; c, the velocity of light; e, the charge of electron; M, the mass of heavy particle (neutral atom or ion).

During inelastic collisions including elementary reactions of excitation, deexcitation, ionization, and recombination, the energy exchange is characterized by the terms

$$Q_n^z = \left[\sum_j \Delta E_{nj}^z (k_{jn}^z N_j^z - k_{nj}^z N_n^z)\right]_{j\in\Omega_n^z} N_e$$

$$\hat{Q}_n^z = I_n^z (\beta_n^z N_e N_0^{z+1} - \alpha_n^z N_n^z) N_e,$$

where Q_n^z takes into account the energy exchange due to reactions of excitation and quenching the level in the atom or ion; $\hat{Q}_n^z$ takes account of the energy exchange due to ionization and three-particle recombination. The value of ionization energy of nth state I_n^z is calculated as $I_n^z = I_z - E_n^z$, where E_n^z is excitation energy of nth level of z-charged particle and I_z is ionization energy of ground state.

Note that in contrast with the energy equation for electrons, the energy balance equation for heavy particles does not include the term dN_g/dt connected with the rate of change in the concentration of heavy particles, since this concentration remains constant under the assumption of the monoatomic plasma of one chemical element.

Thus, the energy balance equations (10) and (11), together with the equations for energy level populations and charge distribution (5) and (9), make a closed system describing the dynamics of processes in the nonequilibrium spatially homogeneous laser plasma.

To estimate quantitatively to what extent the processes are nonequilibrium, solutions of the nonlinear system of differential equations (5)–(11) were compared with equilibrium values of the density of charged (ions and electrons) and of excited particles calculated at the temperatures T_e and T_g. Equilibrium values of the concentrations of ions N_i^z and electrons N_e were determined from the solution of the nonlinear system of Saha equations (*24*),

$$\frac{N_e \Sigma_i N_i^{z+1}}{\Sigma_i N_i^z} = \frac{g_e g^{z+1}}{g^z} \left\{\frac{mT_k}{2\pi\hbar^2}\right\}^{3/2} \exp\left(\frac{-I_z}{T_k}\right); \qquad z = 0, 1, \ldots, z_{\max}; \qquad k = e, g, \tag{12}$$

where g^z is the statistical sum of z-charged ion; g_e, g_n^z, g_0^z, statistical weight of electron, nth state, and ground state of the z-charged ion, respectively. Populations of excited levels were estimated via the ground states, N_0, using the known Boltzmann relations:

$$N_n^z = N_0^z \exp\left(-\frac{E_n^z}{T_k}\right)\frac{g_n^z}{g_0^z} \qquad k = e, g. \tag{13}$$

REACTIONS RATES AND NUMERICAL SOLUTIONS

When constructing the mathematical model, special attention was paid to adequate description of rate coefficients of elementary events. There are several methods of solving this problem. Within the range of high energies of colliding particles $\epsilon \geqslant 100$ eV the calculations of cross-sections using classical and quantum mechanical approaches are in a good agreement with experimental data (*35–38*). Determination of coefficients of rates of elementary reactions in the low energy range $\epsilon < 10$ eV is the most difficult. Here the results of experimental measurements of cross-sections and reaction rates are usually used. But such data are available for a limited number of elementary processes only. Moreover, the values of cross-sections reported in experimental papers largely differ from each other. In the present paper, to calculate rate coefficients, approximation expressions constructed in view of theoretical and experimental studies (*39–44*) are used.

As for coefficients of rates of spontaneous radiative decay of exited levels, either the reference data of (*44, 45*) were used or, if the latter were not available, decay probabilities were determined via the oscillator strengths f_{nm}^z,

$$a_{nm}^z = 8 \times 10^5 \left\{\frac{\Delta E_{mn}^z}{Ry}\right\}^2 \frac{g_n^z}{g_m^z} f_{nm}^z, \qquad [s^{-1}], \tag{14}$$

where f_{nm}^z is the oscillator strength for the transition from the nth state to the mth state in a z-charged particle; ΔE_{mn}^z is the energy difference between the n and m levels; g_n^z, g_m^z are the statistical weights of the m and n atomic levels for the z-charged particle.

If oscillator strengths were not available from the literature, their values were estimated by the hydrogen-like dipole moment $f_{nm}^{z(H)}$

$$f_{nm}^z = f_{nm}^{z,(H)} \frac{g_n^{z,(H)}}{g_m^z} \frac{\Delta E_{nm}^z}{\Delta E_{nm}^{z,(H)}}$$

where the index H denotes the corresponding values in the hydrogen atom or ion. The value ν_{en} is determined via the cross-section σ for elastic collisions of electrons with neutral atoms and the mean velocity of thermal motion of electrons $\bar{v}_e$ (*24*),

$$\bar{v}_e = 6.7 \times 10^7 \sqrt{T_e}, \qquad [\text{cm} \cdot \text{s}^{-1}] \qquad \sigma = \frac{\sigma_0}{\sqrt{T_e}}$$

where $\sigma_0 \simeq 10^{-15}$ cm^2 gas-kinetic cross-section. Thus, we have

$$\nu_{en} = \bar{v}_e \sigma \left[\sum_j N_j^0\right] = 6.7 \times 10^{-8} \left[\sum_j N_j^0\right]_{j \in \Theta^z}, \qquad [\text{s}^{-1}]. \tag{15}$$

The frequency of electron–ion collisions was determined by the formula,

$$\nu_{ei} = 3.64 \times 10^{-6} \ln \lambda T_e^{-3/2} \sum_{z=1}^{z_{max}} z \left[\sum_j N_j^z \right]_{j \in \Theta^z}, \qquad [s^{-1}], \tag{16}$$

where $\ln \lambda$ is the Coulomb logarithm.

The constants of excitation reaction rates for the atom and ion with the z-charge by elecron collison were determined with the help of the Van Regemorter approximation formula (*43*):

$$k_{mn}^z = 1.58 \times 10^{-5} \frac{f_{mn}^z}{\Delta E_{mn}^z \sqrt{T_e}} \exp \left\{ \frac{\Delta E_{mn}^z}{T_e} \right\} q_{mn}^z, \qquad [cm^3 \cdot s^{-1}]. \tag{17}$$

q_{mn}^z is the Mewe factor.

$$q_{mn}^z = A + Cx_{mn}^z + [Bx_{mn}^z - C(x_{mn}^z)^2 + D] \exp \left\{ \frac{\Delta E_{mn}^z}{T_e} \right\} Ei(x_{mn}^z)$$

$$x_{mn}^z = \frac{\Delta E_{mn}^z}{T_e}; \qquad -Ei(-x) = \int_x^\infty \frac{e^{-t}}{t} dt,$$

where Ei is the integral exponent, and the values A, B, C, D are constants determined by the type of electron transition (dipole, quadrapole, etc.), their values being given in (*47*). The inverse value of the level excitation rate was calculated from the relation of detailed balance:

$$k_{nm}^z = k_{mn}^z \frac{g_m^z}{g_n^z} \exp(-x_{mn}^z). \tag{18}$$

The ionization reaction rate coefficient for atoms and ions was calculated with the help of the Lotz formula (*41*)

$$\alpha_n^z = 3.14 \times 10^{-6} \frac{\zeta_n^z Ei(x_n^z)}{T_e^{3/2} x_n^z} \exp(-x_n^z), \qquad [cm^3 \cdot s^{-1}], \tag{19}$$

where $x_n^z = I_n^z/T_e$; ζ_n^z, the number of equivalent electrons in the nth state of z-charged particle.

In the given statement of the problem, three-particle recombination is a reaction reciprocal to collision ionization. The rate coefficient for this reaction is calculated from the detailed balance relation (*34*):

$$\beta_n^z = \alpha_n^z \cdot \frac{g_n^z}{g_e g_0^{z+1}} \left\{ \frac{2\pi\hbar^2}{mT_e} \right\}^{3/2} \exp(x_n^z), \qquad [cm^6 \cdot s^{-1}]. \tag{20}$$

The nonlinear system of differential equations (5)–(11) describes events of different scale whose characteristic times of development differ by several orders. In the general case such systems of equations refer to stiff systems, i.e., systems with solutions containing quickly and slowly changing components. Difficulties involved in solving stiff systems are well known (*48–52*). At present there is a thoroughly developed theoretical basis for devising methods to solve such a system of large dimensions (*50*), including those with variable stiffness (*51*). They are practically realized in various software packages widely used in solving a number of applied problems (*52–55*).

The initial solution of the system was made with the help of a software complex which is a constituent of the LASTEC-4 package of applied programs worked out by the authors to solve problems of nonequilibrium radiative gas dynamics. This program complex is based on one of the modifications of the Gear–Adams methods belonging to the class of multistep methods of the predictor–corrector type. As in (*55*), the program complex allows for automatic selection of an integration step and switching from the Gear stiff method to the Adams nonstiff one.

Systems of Saha nonlinear algebraic equations were solved with the help of a specially worked out iteration procedure with quick convergence (*56*).

ANALYSIS OF MODELING RESULTS

The principal aim of modeling was to study the dynamics and general features of nonequilibrium processes taking place in metal vapors under the action of laser radiation of various intensity.

The dynamics of optical breakdown are conveniently characterized by the relation of the frequencies of electron-neutral and Coulomb collisions (ν_{en} and ν_{ei}, respectively). According to (*57*), a medium with $\nu_{en} \gg \nu_{ei}$ refers to a partially ionized gas and a medium having the inverse relation, $\nu_{en} \ll \nu_{ei}$, is a plasma, i.e., a totally ionized gas. Thus the phenomenon of optical breakdown can be treated as a transition between these two states and is characterized by a sharp increase of ν_{ei} from the initial value that is much less than ν_{en} up to the final value that is much more than ν_{en}.

TABLE I
Levels of Cu Neutral Atom and Ions Taken into Account in the Model

Cu		Cu^+	
$3s^23p^63d^{10}4s$	$(^2S_{1/2})$	$3s^23p^63d^{10}$	$(^2S_0)$
$4s^2$	(^2D)	$4s$	$(^{1,3}D)$
$4p'$	$(^{2,4}P^o,^2F^o,^{2,4}D^o)$	$4p$	$(^1P^o,^{1,3}D^o,^3F^o,)$
$5d$	(^2D)	$5s$	(^3D)
$5s$	$(^2S,^4D)$	$5p$	$(^3D,^3G,^3F,^3F^o,^3P^o)$
$5p$	$(^2P^o)$	$6s$	(^3D)
$6p$	$(^2P^o)$	$3d^{10}8$	
$7p$	$(^2P^o)$	$3d^{10}9$	
$3d^{10}8$		$3d^{10}10$	
$3d^{10}9$			
$3d^{10}10$			

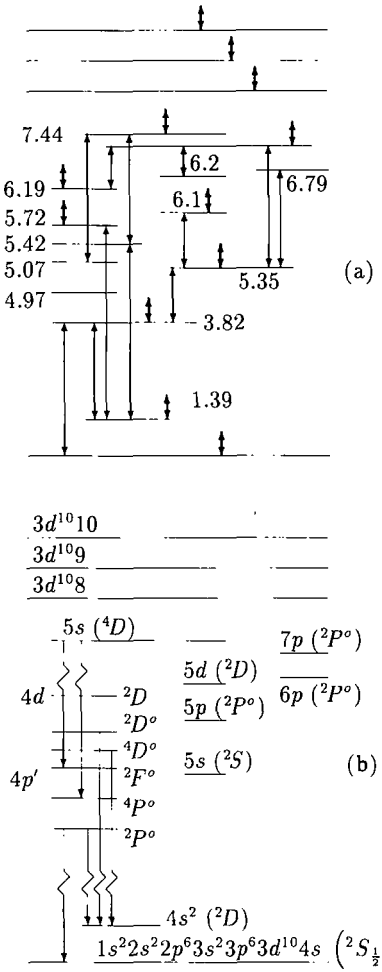

FIG. 1. Diagrams of excited states of Cu neutral atom (ionization potential $I = 7.726$ eV). (a) Radiative transitions between excited states, (b) collision transitions. The processes of ionization and three-particle recombination are indicated by symbols ↕. The values of the level ionization potentials are given in (b).

Optical breakdown of gaseous media is well known to have a pronounced threshold nature as for the intensity and duration of laser action.

Consider the behavior of vapors of copper under the action of laser radiation with the wavelength $\lambda = 1.06\ \mu m$ and near-threshold values of intensity. Initially, the pulse duration was not limited, and the intensity varied within the range $G = 10^6$–10^{10} W/cm^2. The values of radiation intensity G were chosen from the range of values where plasma formation processes were observed experimentally. In calculations the initial values of vapor temperature and density were taken to be the same and typical for the outer side of the Knudsen layer under developed evaporation (*30*):

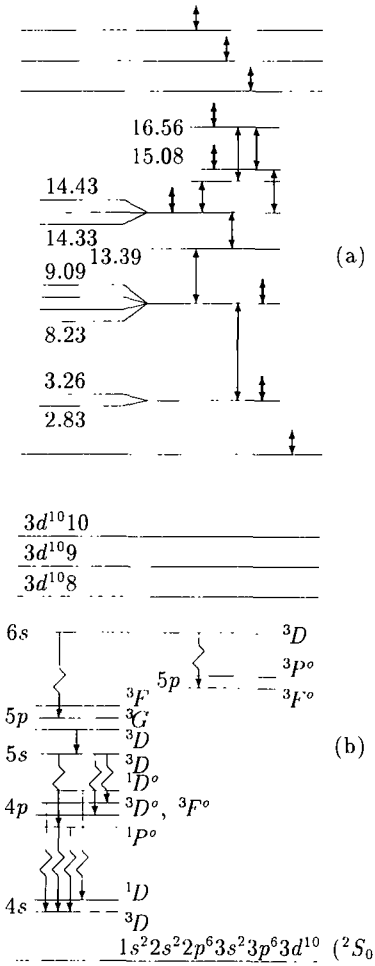

FIG. 2. Diagrams of excited states of Cu^+ ion (ionization potential I = 20.291 eV). (a) Radiative transitions between excited states, (b) collision transitions. Symbols are similar to those in Fig. 1.

$$T^0_{e,g} = 0.2 \text{ eV} \qquad N_0 = 6 \times 10^{18} \text{ cm}^{-3}.$$

These values correspond to the equilibrium density of electrons and ions equal to

$$N_e^{Saha} = 6 \times 10^{11} \text{ cm}^{-3}.$$

The equilibrium density of excited states is determined from relations (*12*) and (*13*).

Prebreakdown Action Regime

Depending on the value of intensity G, the laser radiation interaction with the evaporated material can proceed in two qualitatively different regimes. In the first one, the evaporated material turns into the state of a partially ionized gas with ν_{en}

$> \nu_{ei}$. In the second one, vapors pass into the state of complete or nearly complete ionization with $\nu_{ei} \gg \nu_{en}$.

The first regime is realized at an insufficiently high intensity of radiation. The main features of the development of such regimes in copper vapors at $G = 10^8$ W/cm^2 are illustrated by the temporal dependencies (Figs. 3–5) of excited states of a neutral atom (Fig. 5), the ion Cu^+ component density (Fig. 3), and temperatures of electrons and ions components (Fig. 4).

Let us consider the general pattern of the processes. In the radiation electromagnetic field, electrons gain energy due to the inverse-bremsstrahlung effect and expend it in elastic and inelastic collisions.

The dynamics of kinetic processes can be conditionally separated into three stages.

At the first stage ($t \leqslant 10^{-7}$ s, approximately) the spontaneous radiative decay of excited states is the dominating process. The ionization is weak because of the insufficient rate of energy gain (G is relatively low). Only levels 3, 7, 8 . . . , which can radiatively decay, are depopulated (Fig. 5). Population of levels without radiation transitions remains practically the same.

At the second stage ($t \approx 10^{-7}$–10^{-2} s) the further deexcitation is limited by the considerable heating of electron gas (Fig. 4). The energy released because of deexcitation increases the T_e from 0.2 eV to 0.27 eV. At this stage the energy balance of heavy particles remains practically the same. This leads to the violation of thermodynamic equilibrium, since $T_e > T_g$. The T_e increase leads to the compensation of deexcitation process by collision transitions. Concentrations of all the excited states start to increase slowly. The balance of energy gain and loss in the electron subsystem is established quickly, and the electron temperature remains the same for a comparatively long period. At the middle of the second period the radiation decay of higher levels, as 5, 6, 10 (having low probability of radiation decay), takes place (Fig. 5).

The final stage ($t > 10^{-2}$ s, approximately) is characterized by the intensification of the ionization process. The electron density rapidly increases to about one

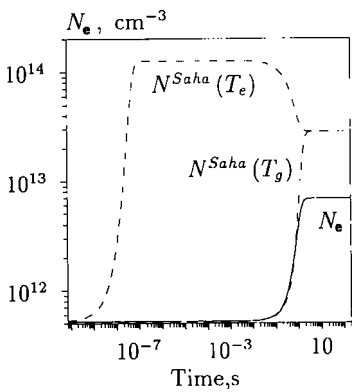

FIG. 3. Concentration of electrons in Cu vapors ($G = 10^8$ W/cm^2). Dashed lines show equilibrium electron concentrations (calculated from the Saha equations) for temperatures T_e and T_g from Fig. 4.

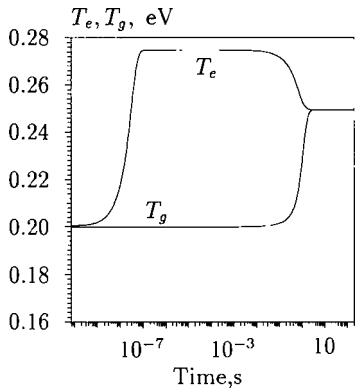

FIG. 4. Temperatures T_e (electrons) and T_g (atoms and ions) in Cu vapors ($G = 10^8$ W/cm^2).

order of magnitude (Fig. 3). At this stage, one can see the equalizing of T_e and T_g. Ionization energy losses and the increased efficiency of elastic scattering (because of N_e increase) equalize the temperature. Decrease of T_e leads to the important intensification of the three-particle recombination process, which results in the increased concentration of all the excited states (Fig. 5).

Upon reaching the thermodynamic equilibrium, the system as a whole attains a stationary state at which all the processes appear to be mutually balanced, unlimited laser action being compensated by a spontaneous radiative decay of excited states. In full-scale experiments this effect can be revealed as a rather powerful radiation flux, which is sometimes erroneously taken to be a laser plasma. Mathematical modeling shows that, if spontaneous transitions are not taken into consideration (i.e., $a_{mn} = 0$), the system (5)–(11) has no stationary solutions. Comparing the obtained equilibrium density values for charged particles N_e, $\Sigma_n N_n^z$ ($z > 1$) (Fig. 3, dashed lines) and excited particles N_n^z ($n > 1$) (Fig.

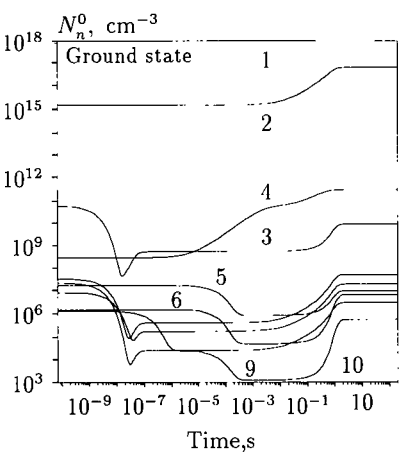

FIG. 5. Concentration of Cu atoms in ground and excited states. The curves going down refer to the energy levels in Table 1. Laser radiation intensity $G = 10^8$ W/cm^2. Initial density of vapor, 6×10^{18} cm^{-3}. Vapor initial temperature, $T_0 = 0.2$ eV.

5) shows that they differ significantly from the Saha–Boltzmann ones found from Eqs. (12). Calculations show that the differences may be of one or two orders of magnitude, depending on the intensity and duration of laser radiation.

Thus, laser action regimes with intensities insufficient for optical breakdown are represented by a complicated pattern of nonequilibrium interconnected processes which are eventually responsible for the optical properties and radiative capability of partially ionized vapors. Although, if the action is long enough and the system comes to thermodynamic equilibrium, its quantitative estimates do not coincide with the Saha–Boltzmann ones because of powerful spontaneous radiation. Thereby the Saha–Boltzmann description turns out to be inadequate to describe optical characteristics of the laser plume.

As the intensity G increases, so do the values of N_e, N_n, T_e, T_g, and ν_{ei}. The relation between the frequencies ν_{en} and νei remains the same, $\nu_{en} \gg \nu_{ei}$ up to $G \sim 10^8$ W/cm^2 (Figs. 6 and 7). At a sufficiently high intensity (2×10^9 W/cm^2) the density of charged particles becomes so high that the frequency of Coulomb collisions becomes compatible with and then quickly exceeds that of electron-neutral collisions ($\nu_{ei} > \nu_{en}$) (Figs. 6 and 7). The radiation intensity at which the frequencies ν_{ei} and ν_{en} become equal can be considered as a lower threshold of breakdown, since any further increase in the intensity G with unlimited laser action duration must result in the relation $\nu_{ei} \gg \nu_{en}$ being fulfilled and the avalanche ionization in vapors being developed. Hereafter, the minimal radiation intensity necessary for an optical breakdown to occur at a given pulse duration will be referred to as an upper breakdown threshold.

Optical Breakdown

The avalanche ionization is characterized by domination of electron excitation and cumulative ionization. By convention it can be divided into two stages. The

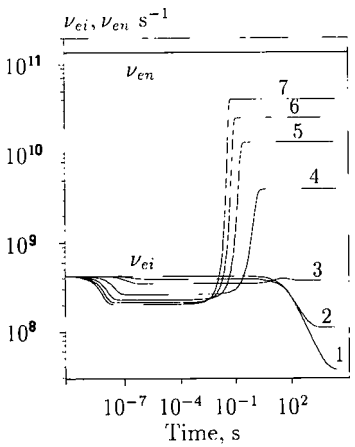

FIG. 6. Frequencies of electron – neutral ν_{en} and electron – ion ν_{ei} collisions in Cu vapors. Initial density of vapor, 6×10^{18} cm^{-3}. Vapor initial temperature $T_0 = 0.2$ eV. The curves correspond to the following laser radiation intensities: 1, $G = 10^6$ W/cm^2; 2, $G = 3 \times 10^6$ W/cm^2; 3, $G = 10^7$ W/cm^2; 4, $G = 10^8$ W/cm^2; 5, $G = 3 \times 10^8$ W/cm^2; 6, $G = 5 \times 10^8$ W/cm^2; 7, $G = 7 \times 10^8$ W/cm^2.

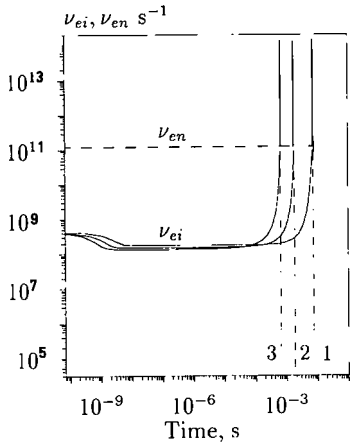

FIG. 7. Frequencies of electron – neutral ν_{en} and electron – ion ν_{ei} collisions in Cu vapors. Initial density of vapor 6×10^{18} cm^{-3}. Vapor initial temperature $T_0 = 0.2$ eV. The curves correspond to the following laser radiation intensities: 1, $G = 2 \times 10^9$ W/cm^2; 2, $G = 5 \times 10^9$ W/cm^2; 3, $G = 10^{10}$ W/cm^2.

first stage involves a relatively slow process of filling the excitation levels, and the second stage is characterized by their violent ionization. At the beginning of the first stage, electrons colliding mainly with neutral atoms ($\nu_{ei} \ll \nu_{en}$) rapidly gain energy in the laser radiation field. Energy exchange between the electron subsystem and heavy particles is made difficult because of the great difference between the mass of an electron, m, and that of atom, M, $m/M \sim 10^{-4}$–10^{-5} and the electron temperature T_e at this stage is much higher than the vapor temperature T_g (Fig. 8). At this stage nearly all the electron energy is expended to fill the levels.

Ionization losses are not great because of the low rate of ionization limited by the value of the electron temperature $T_e \ll 1$ eV. As long as the relation $\nu_{en} \gg \nu_{ei}$ is fulfilled, the electron temperature does not change, because acquisition of energy by electrons is compensated by excitation losses. As the density of excited states and charged particles increases, so does the frequency of Coulomb colli-

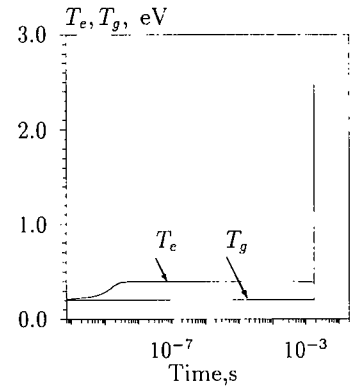

FIG. 8. Temperatures T_e (electrons) and T_g (atoms and ions) in Cu vapors ($G = 5 \times 10^9$ W/cm^2).

sions. This is the slowest stage of avalanche ionization. Once the value ν_{ei} becomes compatible with the frequency of electron-neutral collisions, the electron temperature begins to grow rapidly. The avalanche ionization enters the fast stage at which the energy exchange between the subsystems is accelerated. Figure 9 shows the evolution of charged particles (electrons) in copper vapors at $G = 2 \times 10^9$ W/cm^2. At such an intensity the maximum electron temperature can be as high as ~3 eV, which is sufficient for the total ionization of neutral atoms and singly or doubly ionized particles.

If the intensity is not very high, $G < 3 \times 10^7$ W/cm^2, the temperature value becomes stationary. At high intensities, due to a limited number of ions taken into account by the model, the temperature can rise indefinitely. For both substances the temporal dependencies of the concentrations of electrons and ions calculated by the kinetic model are compared with the equilibrium values found for the two temperatures T_e and T_g from the Saha equations. Comparison shows that the curves determined by the kinetic model lie between two equilibrium curves N_e^{Saha} (T_e) and N_e^{Saha} (T_g) at $T_e \neq T_g$ and completely coincide when the temperatures become equal $T_e \simeq T_g$.

Thus, comparison of the curves $N_e(t) = \Sigma_{i,z} N_i^z$, $N_e^{Saha}(T_e)$ and $N_e^{Saha}(T_g)$ points to strongly nonequilibrium avalanche ionization. In the optical breakdown regime, radiative transitions are of little significance, since the frequency of Coulomb collisions, ν_{ei}, is much higher than that of electron-neutral collisions ($\nu_{ei} \gg \nu_{en}$) and that of the spontaneous decay of excited states ($\nu_{ei} \gg \alpha_{nm}^z$). Therefore, once the system reaches thermodynamic equilibrium, the plasma charge composition agrees completely with the Saha–Boltzmann distribution.

Mathematical modeling shows that the closer the excited states are to the ground state, the shorter the breakdown time and the lower the intensity threshold values. Thus, as the excitation energy of the resonance level decreases by 1 eV, the threshold intensity decreases to 7×10^8 W/cm^2, i.e., about three times. Decreasing the ionization potential of a copper atom down to 6 eV also causes threshold values of G and breakdown times to be reduced. It should be noted that

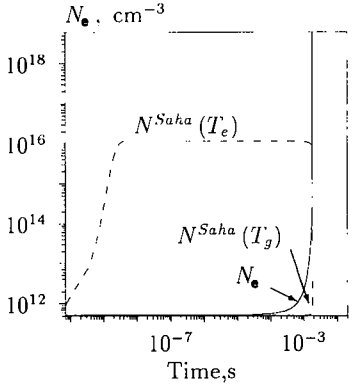

FIG. 9. Concentration of electrons in Cu vapors ($G = 5 \times 10^9$ W/cm^2). Dashed lines show equilibrium electron concentrations (calculated from the Saha equations) for temperatures T_e and T_g.

the simultaneous shift of several levels may give the opposite result. Therefore, the influence of electronic state distribution of neutral atoms on optical breakdown threshold should be analyzed in detail in the future. In particular, the comparison between different elements is rather promising.

Temperature and Temporal Dependence of Optical Breakdown

Let us consider the influence of two main parameters of optical breakdown, namely, the initial temperature $T_e(t) \mid_{t=0} = T_g \mid_{t=0} = T_0$ and the pulse duration τ.

As the initial temperature, T_0, grows, the vapor ionization enhances initial concentrations of charged particles and, hence, the frequency ν_{ei} increases. In this way the relation $\nu_{ei} \gg \nu_{en}$ is achieved at considerably lower values of the threshold intensity G.

As the initial vapor temperature T_0 rises from 0.2 to 0.4 eV, the value of the lower breakdown threshold becomes 2–10 times smaller (Fig. 10). At temperatures $T_0 = 0.4$ eV the initial frequency of Coulomb collisions is found to be higher than the frequency of electron-neutral collisions $\nu_{ei} > \nu_{en}$, i.e., from the very beginning the evaporated substance is already in a plasma state. For a new equilibrium state to be established in such situations, much shorter times and smaller intensities are required. Depending on the intensity applied, the breakdown duration at $T_0 = 0.4$ eV is shifted from the millisecond range to the micro- or nanosecond range. On the other hand, for breakdown to occur, a decrease in the pulse duration would require the radiation intensity to be increased above the threshold value. Thus, the curves shown in Fig. 10 represent the upper threshold values of intensity depending on the laser pulse duration.

CONCLUSION

The collision-radiation model used in the simulation of copper vapor heating by laser pulse includes the kinetics of excitation/deexcitation and the ionization/

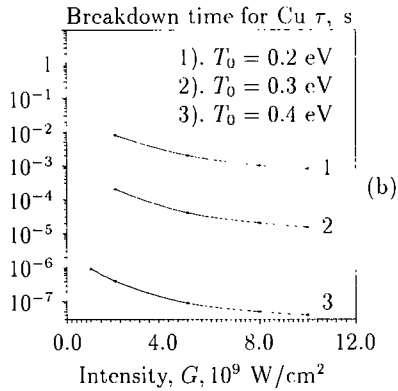

FIG. 10. Dependence of breakdown time for Cu vapor on laser radiation intensity for different initial temperatures, T_0.

three-particle recombination process. The model considers the neutral Cu atom, the first ion Cu^+ and the second ion Cu^{2+} (the last one in the form of a core).

Nonequilibrium phenomena should be taken into account in laser radiation interaction with copper vapor at prebreakdown and at breakdown regimes. These phenomena are important for determining the optical and out-of-equilibrium thermodynamic parameters of the vapor.

If the radiation intensity is smaller than necessary for initiating an electron avalanche, then, in the case of long pulse duration, the system comes to a stationary state characterized by one temperature; the equilibrium between the radiation and the vapor is absent. The temperature between the electron and the heavy particles subsystems may differ by 20–50%; the time for the temperatures to equalize is in the range of 10^{-3}–10^{-1} s for $G = 5 \times 10^7$–10^9 W/cm^2. The charged particle concentrations differ from those of Saha–Boltzmann by a factor ranging from 2 to 10. The absence of equilibrium makes the Saha–Boltzmann distribution inadequate to estimate quantitatively the optical characteristics of the laser plume.

Optical breakdown of copper vapor is essentially the nonequilibrium transition state from a partially ionized vapor ($\nu_{ei} \ll \nu_{en}$) to a completely ionized plasma ($\nu_{ei} \gg \nu_{en}$). The nonequilibrium character of the process is determined by rapid radiation energy absorption by the electronic subsystem and slow energy exchange with the heavy-particle subsystem. The temperature between the electron and the heavy-particle subsystems may differ by 200–300%, i.e., up to several thousands degrees; the time for the temperatures to equalize is in the range of 5×10^{-8}–10^{-2} s for $G = 2 \times 10^9$–10^{10} W/cm^2.

The strong dependence of the breakdown period and threshold intensity versus initial vapor temperature is shown. The increase of initial temperature from 0.2 to 0.4 eV decreases the breakdown period to about four orders of magnitude. The increase of radiation intensity from 2×10^9 to 10^{10} W/cm^2 ($\lambda = 1.06$ μm) decreases the breakdown period to about one order of magnitude for the fixed initial temperature of the vapor.

REFERENCES

1. Smurov, I.; Uglov, A.; Matterazzi, P.; Miani, F.; Tosto, S. Laser-plasma synthesis of nitride and carbide layers on the surface of refractory metals. In "Proceedings of the 10th International Symposium on Plasma Chemistry, Bochum, Germany, August 4–9, 1991," pp. 1–6.
2. Mazhukin, V.; Smurov, I.; Flamant, G. *J. Comput. Phys.*, 1994, **111**, 78–90.
3. Cottel, C. M.; Grabowski, K. S. *MRS Bull.*, 1992, **27**(2), 44–53.
4. Cheung, J.; Horwitz, J. *MRS Bull.*, 1992, **27**(2), 30–43.
5. Uglov, A.; Gnedovetch, A.; Kulbatchkiy, E. *DAN SSSR*, 1988, **303**(6), 1374–1377. (In Russian.)
6. Polak, L. S.; Ovsjannikov, A. A.; Slovetskii, A. A.; Wursel, F. B. *Theoretical and Applied Plasmochemistry*. Nauka, Moscow, 1975.
7. Tönshoff, H. K.; Overmeyer, L.; Von Alvensleben, F. Laser treatment of materials. *In* "Proceedings of the 4th European Conference on Laser Treatment of Materials, ECLAT'92 (B. L. Mordike, ed.), pp. 21–26. Göttingen, Oberursel: DBM.
8. Green, J. M.; Silfvast, W. T.; Wood, O. R. *J. Appl. Phys.*, 1977, **48**, 2753–2761.
9. Humphries, M.; Kahbert, H. J.; Pippert, K. *The Excimer Laser on Its Way to Industrial Application: Laser in Manufacture*. Springer, London, 1987.
10. Danilov, E. D.; Danilychev, V. A.; Dolgykh; Zvorykin, V. D.; Zaiskov, E. M.; Kerimov; Meteveli, G. E.; Tatanyan, G. Yu, *Quantum Electron.*, 1988, **15**, 2568–2577. (In Russian.)

11. Weyl, G. M.; Rosen, D. I. *Phys. Rev. A.*, 1985, **31**, 2300–2313.
12. Kadawa, K.; Yokoi, S.; Nakajima, S. *Opt. Commun.*, 1983, **45**, 261–265.
13. Radziemski, L. J.; Cremers, D. A.; Niemezyk, T. M. *Spectrochim. Acta, Part B*, 1985, **40**(3), 517–525.
14. Shah, P.; Armstrong, R. L.; Radziemski, L. J. *J. Appl. Phys.*, 1989, **65**(65), 2946–2950.
15. Vaskovsky, Yu. M.; Gordeeva, I. A.; Rovinsky, R. E.; Shirokova, I. P. *Quantum Electron.*, 1991, **18**, 1085–1088. (In Russian.)
16. Shah, P.; Biswas, A.; Armstrong, R. L.; Radziemski, L. J. *J. Appl. Phys.*, 1990, **68**(8), 3809–3813.
17. Weyl, G.; Pirri, A.; Root, R. *AIAAJ*, 1981, **10**, 460–469.
18. Mazhukin, V. I.; Uglov, A. A.; Chetvertushkin, B. N. *Quantum Electron.*, 1983, **10**, 697–701. (In Russian.)
19. Rosen, D. I.; Hastings, D. E.; Weyl, G. M. *J. Appl. Phys.*, 1982, **53**, 5882–5890.
20. Rosen, D. I.; Mitteldorf, J.; Kothandarama, G., *et al. J. Appl. Phys.*, 1982, **53**, 3190–3196.
21. Smirnov, B. M. *Plasma Chem. Plasma Process.*, 1992, **12**, 177–188.
22. Post, D. E., *et al. At. Data Nucl. Tables*, 1977, **20**, 397.
23. Griem, H. R. *Plasma Spectroscopy*, McGraw–Hill, New York, 1964.
24. Zel'dovich, Ya. B.; Raizer, Yu. P. *Physics of Shock Waves and High-Temperature Gas-Dynamical Phenomena*. Nauka, Moscow, 1966. (In Russian.)
25. Holstein, T. *Phys. Rev.*, 1947, **72**, 1212–1215.
26. Biberman, L. M.; Vorobjev, V. S.; Yakubov, I. T. *Kinetics of Nonequilibrium Low-Temperature Plasma*. Nauka, Moscow, 1982. (In Russian.)
27. Derzhiev, V. I.; Zhydkov, A. G.; Yakovlenko, S. I. *Radiation of Ions in Nonequilibrium Dense Plasma*. Energoatomizdat, Moscow, 1986. (In Russian.)
28. Rykalin, N. N.; Uglov, A. A.; Zuev, I. V.; Kokora, A. N. *Laser and Electron-Ray Treatment of Metals*. Mashinostroyenie, Moscow. (In Russian.)
29. Pirri, A. N.; Root, R. G.; Wu, P. K. S. *AIAA J.*, 1978, **16**, 1296–1304.
30. Knight, C. J. *AIAA J.*, 1977, **17**, 519–523.
31. Gudzenko, L. I.; Yakovlenko, S. I. *Plasma Lasers*. Atomizdat, Moscow, 1978. (in Russian.)
32. Stupitsky, E. L.; Lubchenko, O. S.; Rhudaverdyan, A. M. *Quantum Electronics*, 1985, **12**, 1038–1056. (In Russian.)
33. Moore, Ch. E. *Atomic Energy Levels*. Vol. 1. NBS, Washington DC. 1971.
34. Venugopalan, M., ed. *Reactions under Plasma Conditions*, Vol. 1. Western Illinois University, New York, 1971.
35. Webster, D. L.; Hansen, W. W.; Dubeneck, F. B. *Phys. Rev.*, 1933, **43**, 839–844.
36. Drawin, H. W. Collisions and transport cross-sections. In *Plasma Diagnostic* (W. Lochte-Holtgreven, ed.), pp. 842–859. North-Holland, Amsterdam, 1968.
37. Presnyakov, L. P.; Vronov, A. M. *J. Appl. Phys. At. Mol. Phys.*, 1975, **138**, 1280–1288.
38. Vainshtein, L. A.; Sobelman, I. I.; Yukov, E. A. *Atoms Excitation and Expansion of Spectra Lines*. Nauka, Moscow, 1979. (In Russian.)
39. Bazylev, V. A.; Chibisov, M. I. *UFN*, 1981, **133**, 617–643. (In Russian.)
40. McWhirter, R. W. P.; Hearn, A. G. *Proc. Phys. Soc.*, 1963, **82**, 641–654.
41. Lotz, W. *Z. Physik*, 1970, **232**, 101–118.
42. Lotz, W. *Astrophys. J. Suppl.*, 1967, **14**, 207–214.
43. Van Regemorter, H. *Astrophys. J.*, 1962, **132**, 906.
44. Allen, C. W. *Astrophysical Quantities*. The Athlone Press, London, 1973.
45. Zaidel, A. I.; Prekof'ev, V. K.; Raisky, S. M. *Tables of Spectral Lines*. Nauka, Moscow, 1977. (In Russian.)
46. Wiese, W. J.; Smith, M. W.; Miles, B. M. *Transition Probabilities*, Vol. 2. NBS, Washington DC, 1969.
47. Mewe, R. *Astron. Astrophys.*, 1972, **20**, 256–277.
48. Gear, C. W. *Math. Comput.*, 1967, **21**, 146–156.
49. Byrne, C. D.; Hindmarsh, A. C. *J. Comput. Phys.*, 1987, **70**, 1–62.
50. Hairer, E.; Norsett, S. P.; Wanner, G. *Solving Ordinary Differential Equations*. 1. *Nonstiff Problems*. Springer-Verlag, Berlin, 1989.

51. Hairer, E.; Norsett, S. P.; Wanner, G. *Solving Ordinary Differential Equations*. 2. *Nonstiff Problems*. Springer-Verlag, Berlin, 1991.
52. Gear, C. W. *Com. Assoc. Comput. Machinery*, 1971, **14**, 185–190.
53. Hindmarsh, A. C.; Byrne, C. D. Applications of EPISOD: An experimental package for the integration of systems of ordinary differential equations. In *Numerical Methods for Differential Systems* (L. Lapidus and W. E. Schiesser, eds.). Academic Press, San Diego, 1976.
54. Hindmarsh, A. C. *ACM-SIGNUM Newslett.*, 1980, **15**, 10–11.
55. Petzold, L. R. *SIAM J. Sci. Stat. Comput.*, 1983, *1*, 136–148.
56. Shirkov, P. D. *Math. Model. J.*, 1991, **3**, 6–12. (In Russian.)
57. Mitchner, M.; Kruger, C. H. *Partially Ionized Gases*. Wiley, New York, 1973.